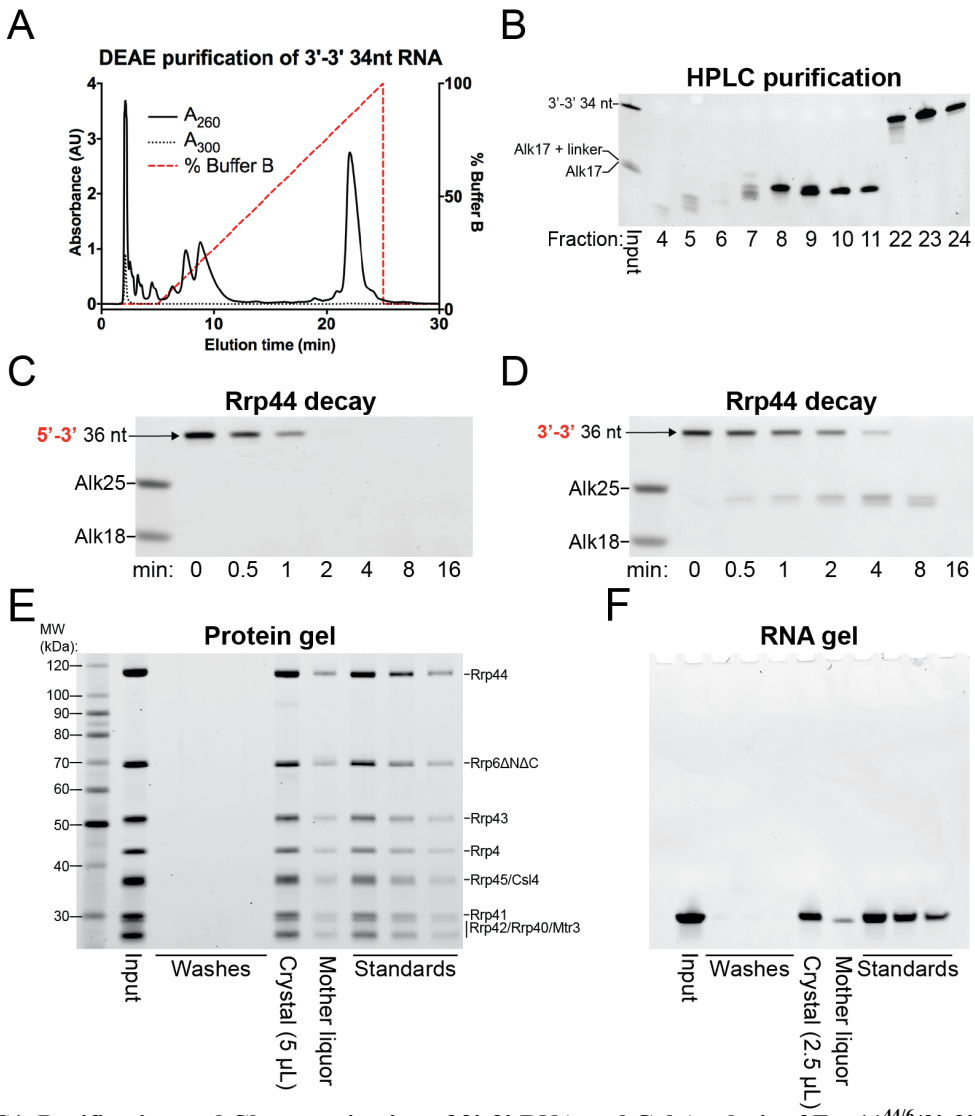

Figure S1. Purification and Characterization of 3'-3' RNA and Gel Analysis of Exo11$^{44/6}$/3'-3' RNA Crystals - Related to Figure 1.

(A) Chromatograms from DEAE separation of an RNA click reaction using an NaCl gradient. Buffers A and B are described in Supplementary Experimental Procedures. For this experiment, 135 µg of total RNA was loaded in a volume of 500 µL. (B) 15% polyacrylamide TBE-urea gel of fractions, which were taken every minute from the HPLC run in (A). RNA is visualized using SYBR gold stain. (C and D) Rrp44 decay time courses on 5'-3'(C) or 3'-3' (D) 36 nt AU-rich RNA substrates. Rrp44 is at a concentration of 5 nM and substrate RNA is at a concentration of 50 nM. Decay intermediates apparent between the alkynyl 25 and alkynyl 18 marker in panel C indicate that Rrp44 cannot degrade through the di-triazole linker. RNA is visualized using SYBR gold staining. (E and F) ~10 crystals were transferred from the mother liquor into three separate 2 µl drops of well solution (washes) and then dissolved in 20 µL of 20 mM Tris-Cl pH 8.0, 100 mM NaCl 1 mM TCEP-HCl. Volumes in the 'Crystal' lane indicate how much of this solution was loaded in that lane. For the protein gel (E), 10µL of dissolved crystal solution was added to 5 µl of 4x loading dye and 5 µL of ultrapure water and 10 µL of that solution was run on a 4-12% acrylamide BIS-TRIS run in MOPS-SDS buffer and stained with SYPRO Ruby. Standards are 1.3, 0.65 and 0.32 pmol of purified complex. For the RNA gel (F), 5 µL crystal solution was added to 5 µL 10 mM Tris-Cl pH 8.0, 0.2 % w/v SDS, 10 mM EDTA, 0.1 U/µL proteinase K and incubated at 50°C for 10 minutes. Following this incubation, 10 µL of 2x urea-PAGE loading buffer was added and 10 µL of that was run on a 15% acrylamide TBE-urea gel. Standards are 1.2, 0.59, and 0.29 pmol of RNA. Quantification of Rrp44 and RNA bands yields an approximate protein:RNA molar ratio of 1:1.3.

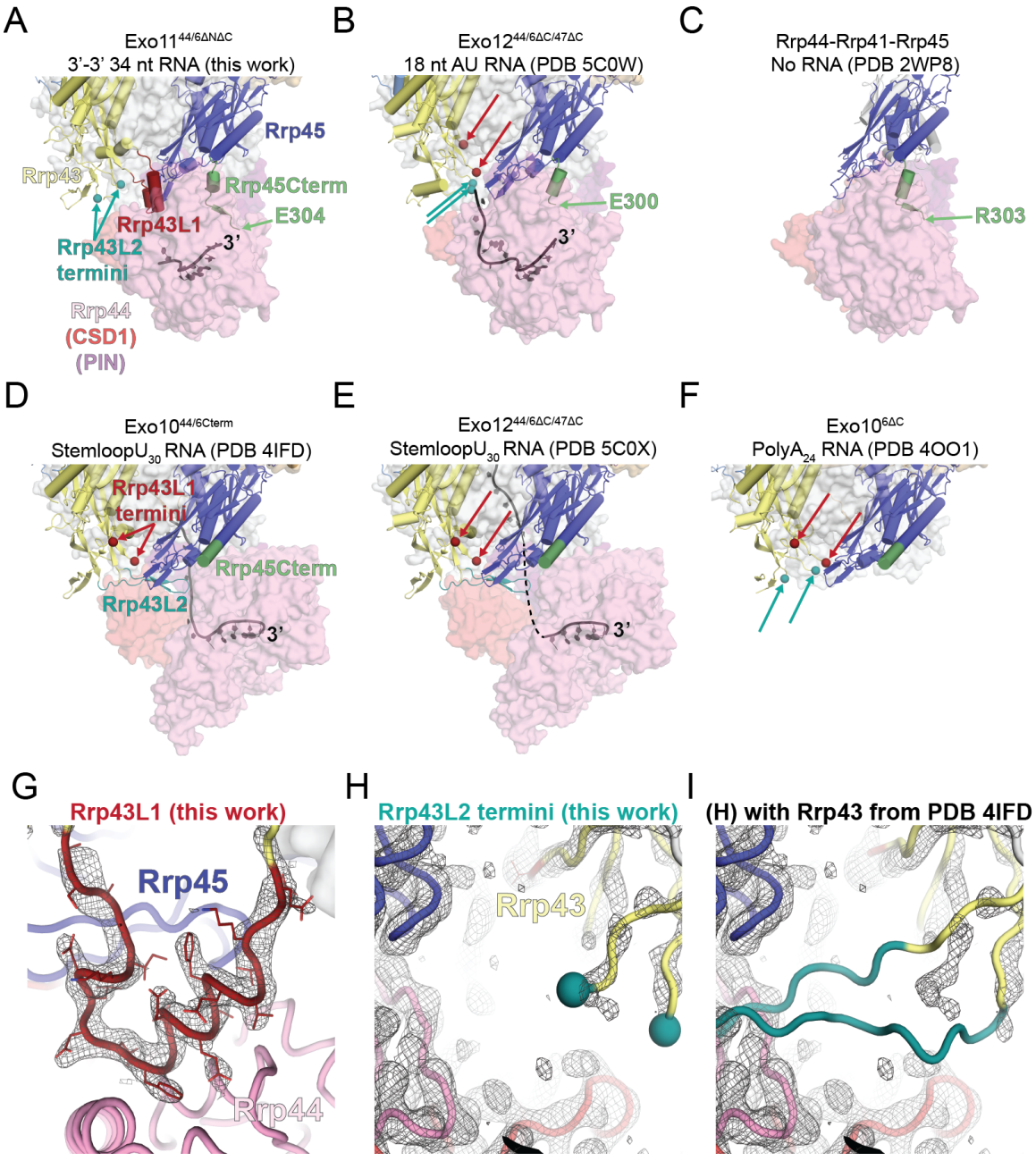

Figure S2. Order-Disorder Transitions in Rrp43 Features and Rrp45$_{Cterm}$ - Related to Figure 2
(A through F) Structures were aligned based on the Rrp43 and Rrp45 chains or, in panel C, only Rrp45. RNase PH-like subunits Rrp41, Rrp46, Rrp42, and Mtr3 subunits are shown as a transparent gray surface for clarity. Terminal residues modeled for Rrp43L1 and Rrp43L2 features are shown as spheres and highlighted with arrows in the channel-dependent (D and E) and channel-independent (A, B and C) conformations, respectively. The dashed line in panel E indicates the presumed RNA path in that structure. (G) Rrp43L1 in the Exo11$^{44/6}$ structure. Mesh is a simulated annealing $2F_o - F_c$ map contoured at 1.5 σ and carved to within 3 Ångstroms of Rrp43. (H) Rrp43L2 termini in the Exo11 structure. Mesh is a simulated annealing $2F_o - F_c$ map contoured at 1.0 σ. (I) Panel H with Rrp43 from the Exo10^{44} structure (PDB: 4IFD) aligned to the Rrp43 chain of Exo11$^{44/6}$ with electron densities shown as in panel H.

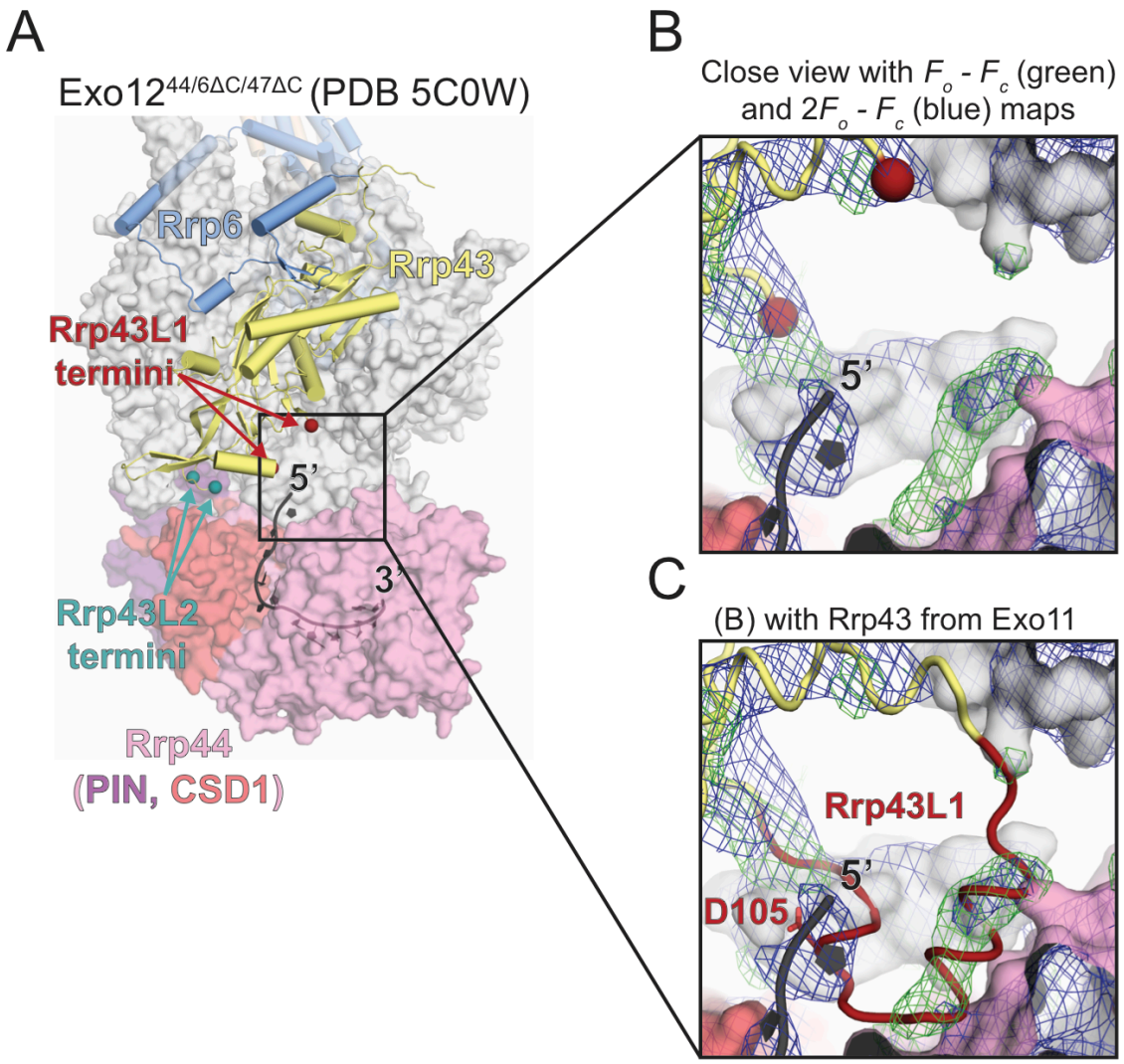

Figure S3. Rrp43L1 Clashes With the 5' end of Rrp44 Bound RNA from the Exo12$^{44/6/47}$ Model - related to Figures 2, 3 and 4

(A) Orientation of Exo12$^{44/6/47}$ used in analysis. (B) Close-up of RNA 5' end with $F_o - F_c$ map shown as green mesh contoured at 2.0 σ and $2F_o - F_c$ map shown as blue mesh contoured to 1.0 σ. Rrp43 residues Thr99 and Asn126, the boundaries of Rrp43L1 in that model, are shown as spheres. Maps were generated in Phenix using the twin operator -h,-k, l. (C) The same view as in (B) but with Rrp43 replaced with Rrp43 from the Exo11$^{44/6}$ structure presented in this work. Alignment was performed based on the Rrp43 chain.

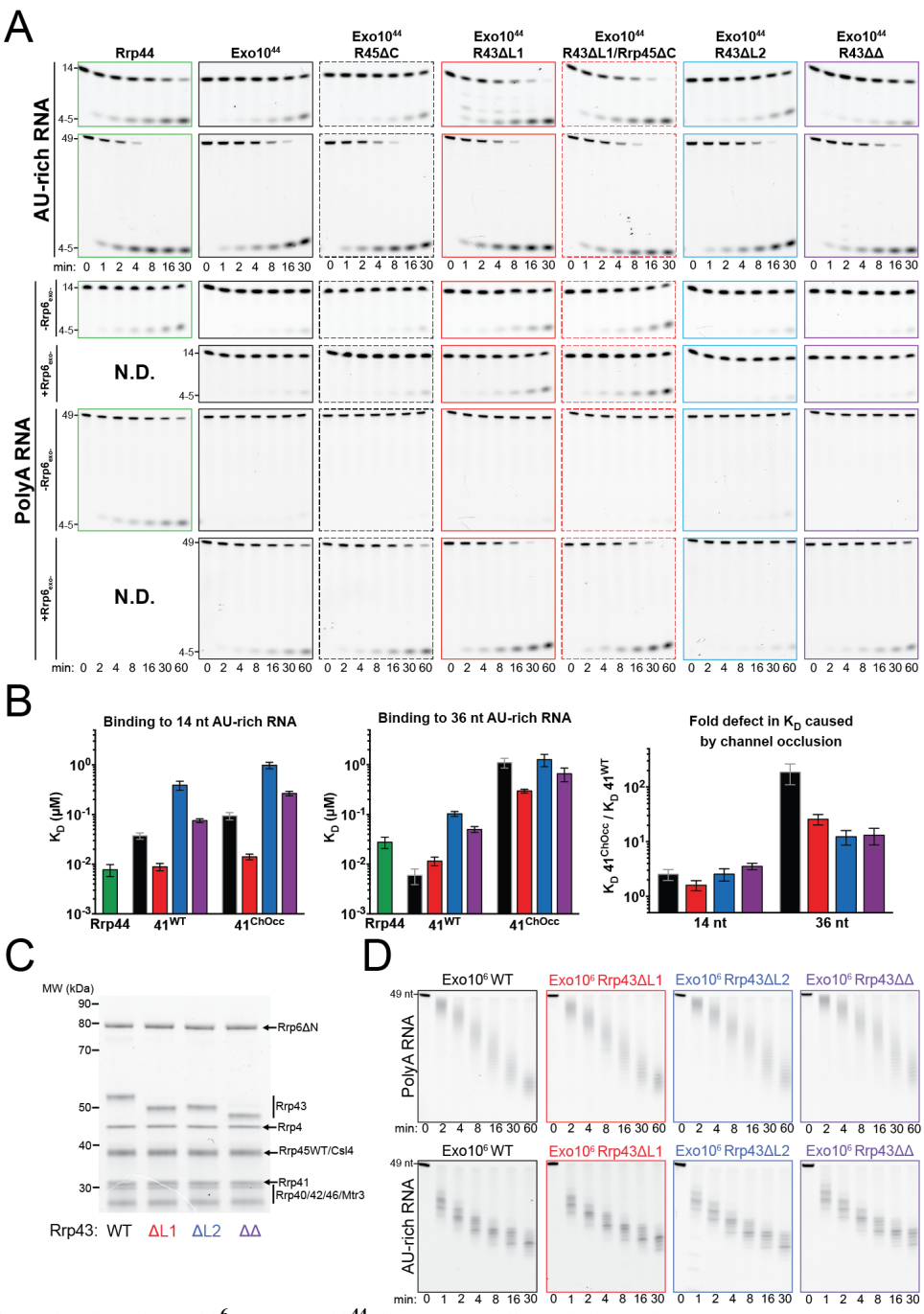

Figure S4. Activities of Exo10^{6} and Exo10^{44} Complexes Containing Wild-Type and Mutant Rrp43 and Rrp45 Proteins - related to Figures 3 and 4

(A) 15% polyacrylamide TBE-urea gel analysis of Exo10^{44} decay activity on 5' FAM 14 nt and 49 nt AU-rich and poly(A) RNAs. Where indicated, a 3-fold molar excess (3 nM final concentration) of a catalytically inactive Rrp6 protein (residues 129-733, D238N mutant) was added to the reaction. The full length RNA substrate is indicated with 14 nt or 49 nt marker and the Rrp44 decay product is indicated with the 4-5 nt marker. N.D. indicates panels that were not done. (B) Binding affinities of Exo10^{44} complexes and free Rrp44 for AU-rich RNA as measured by fluorescence anisotropy. '41^{ChOcc}' refers to a mutant in Rrp41 that occludes the central channel. Mean values of a triplicate experiment are shown with error bars at ±1 SD. (C) SDS-PAGE analysis of reconstituted Exo10^{6} complexes containing deletions in Rrp43. Gel is 4-12% acrylamide BIS-TRIS run in MOPS-SDS buffer and stained with SYPRO ruby. (D) 15% polyacrylamide TBE-urea gel analysis of Exo10^{6} activity on 5' FAM poly(A) and AU-rich 49 nt RNA.

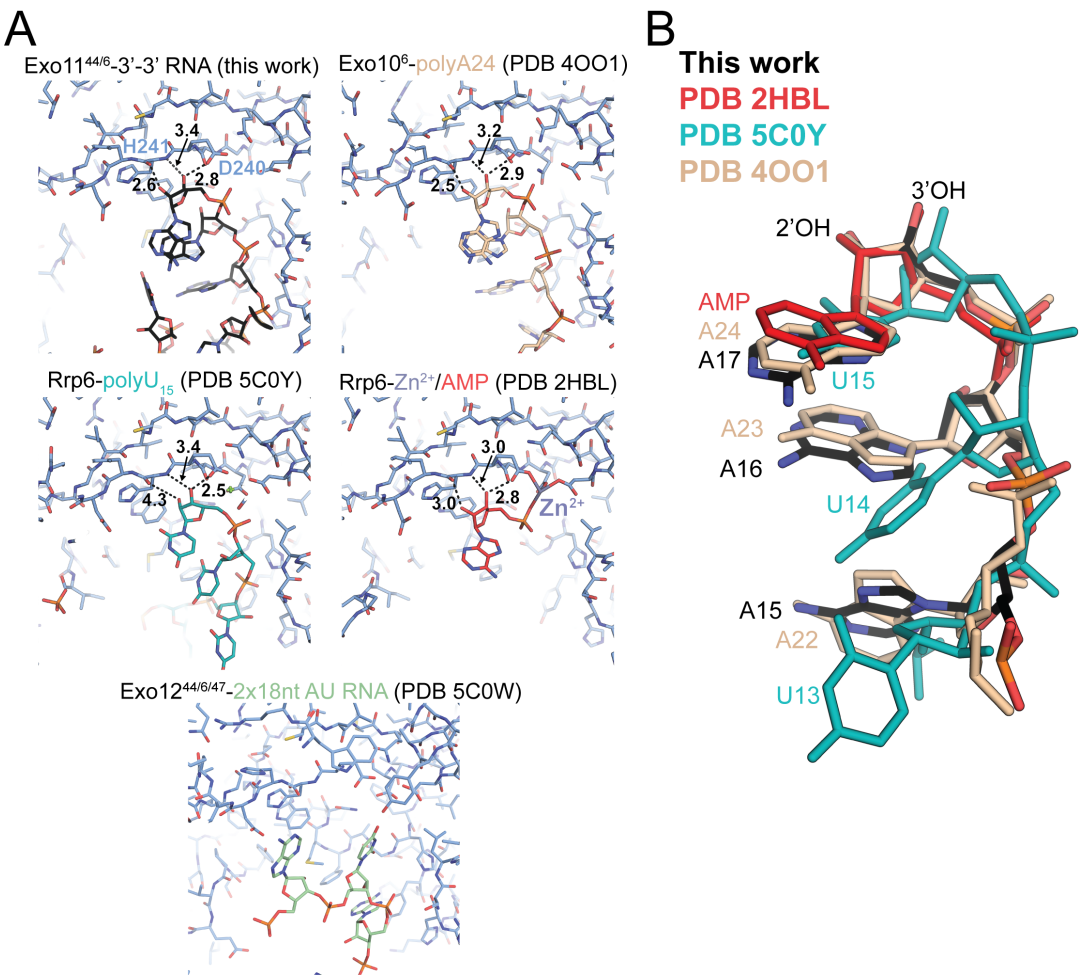

Figure S5. RNA In Proximity to the Rrp6 Active Site - related to Figures 5 and 6
(A) RNA in or near the active site of Rrp6 in several structures in the PDB. Distances to the backbone carbonyl and amide of His241 and side chain of Asp240 are shown in Ångstroms. (B) The three terminal nucleotides of RNA or AMP in the Rrp6 active site from four different structures. Rrp6 residues 150-300, which span the catalytic residues, were aligned and the protein is removed for clarity.

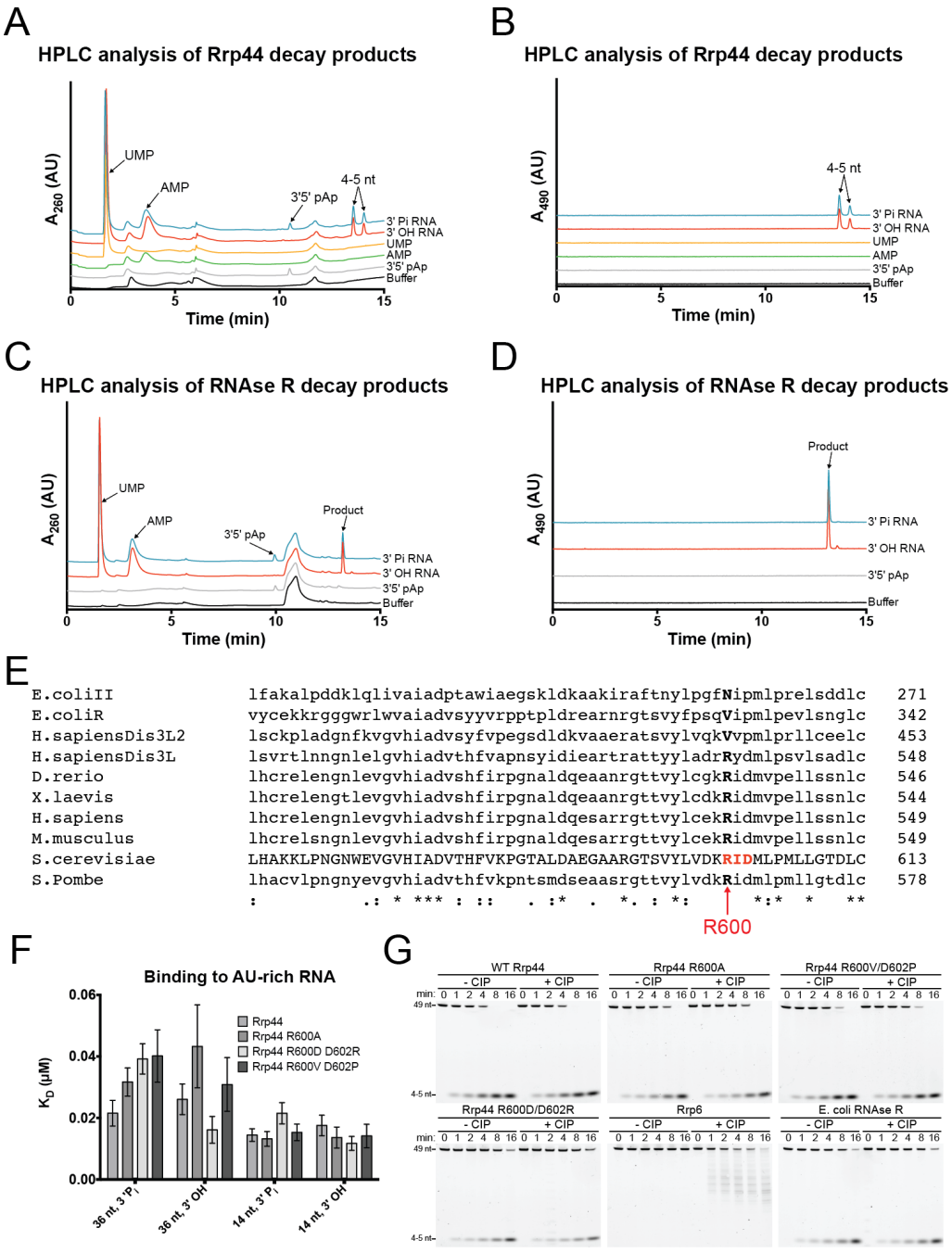

Figure S6. Analysis of Rrp44 Activity on 3' Phosphate RNA - related to Figure 5.
(A through D) Ion-pair reverse phase HPLC analysis of RNA decay products. Reactions contained either Rrp44 (A and B) or *E. coli* RNAse R (C and D) and the indicated substrates. UV absorbance was monitored at 260 nm for detection of nucleotides (A and C) or 490 nm for detection of the 5' fluorescein label (B and D). (E) Multiple sequence alignment using Clustal Omega (Sievers et al., 2011) of Rrp44 (Dis3) from six organisms as well as the related enzymes Dis3L and Dis3L2 from human and RNase II and RNase R from *E. coli*. (F) RNA decay of 3' phosphate 5' FAM 49 nt AU-rich RNA by the indicated enzymes. (G) Binding affinities of wild type and mutant Rrp44 for AU-rich RNA as measured by fluorescence anisotropy. Mean values of a triplicate experiment are shown with error bars at ±1 standard deviation.

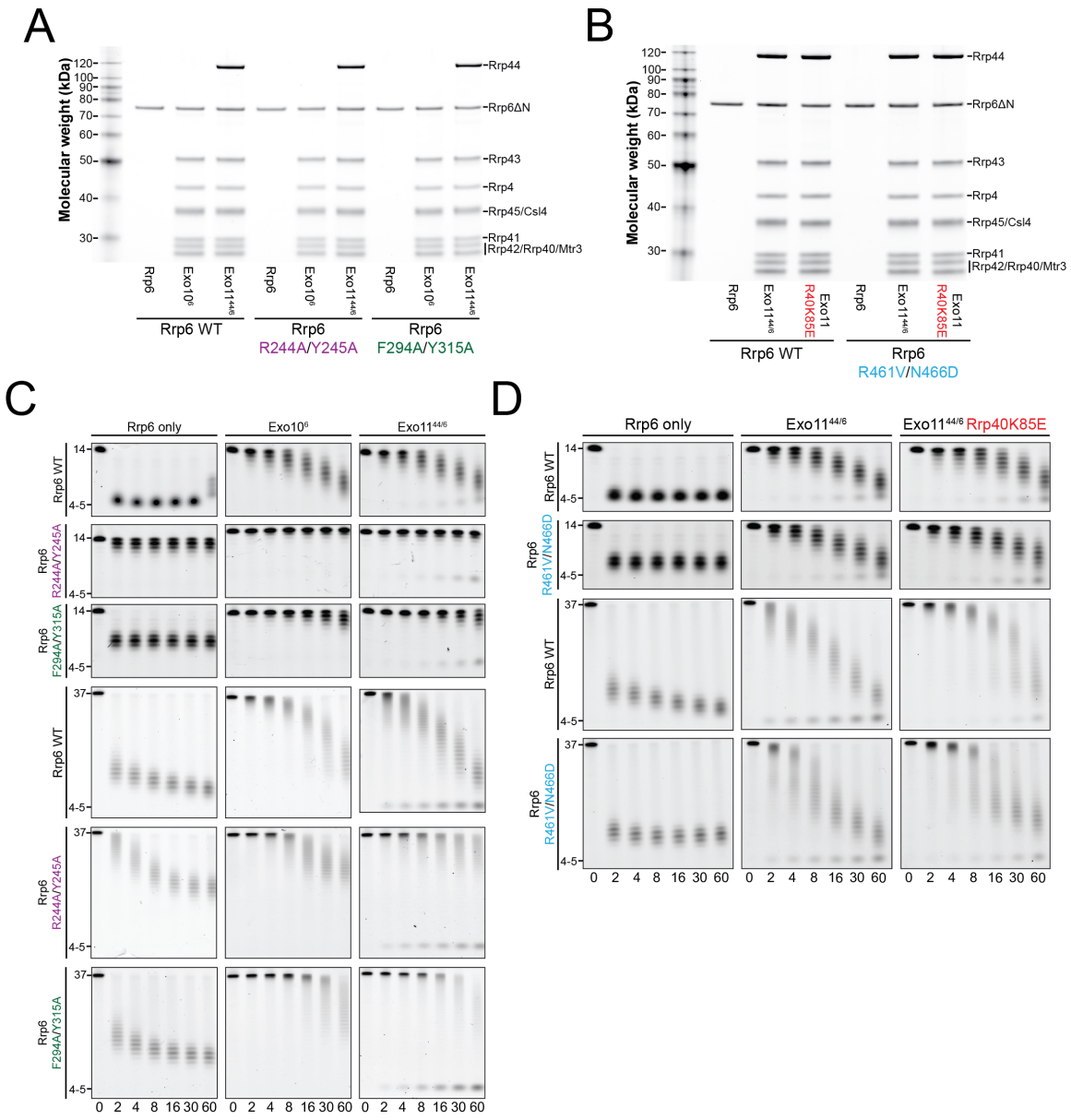

Figure S7. Rrp6 Activity is Diminished by Mutating Non-Catalytic Residues in its Exo Domain and both Rrp6 and Rrp44 Activities are Diminished by a Mutation in the S1/KH Protein Rrp40 - Related to Figure 6

(A and B) SDS-PAGE analysis of Rrp6 wild type and mutant enzymes and reconstituted complexes. Gel is 4-12% acrylamide BIS-TRIS run in MES-SDS running buffer and stained with SYPRO ruby. (C and D) Polyacrylamide TBE-urea analysis of decay time courses of free Rrp6 and reconstituted complexes on 5' FAM poly(A) 14 nt and 37 nt RNA.

Supplemental Experimental Procedures

Expression, and purification of proteins

Saccharomyces cerevisiae Exo9 components were expressed and reconstituted into complexes as described previously (Greimann and Lima, 2008). For reconstitution of complexes containing catalytic subunits, Exo9 cores were mixed with a 3-fold molar excess of Rrp6 and/or 1.5-fold molar excess of Rrp44, incubated at 4°C for 2-4 hrs, and separated from free enzymes using a Superdex200 increase 10/300 GL column (GE) in 20 mM Tris-Cl pH 8.0, 100 mM NaCl, 0.1 mM $MgCl_2$, 0.5 mM TCEP-HCl. All preparations of Rrp6 in this work lack the N-terminal 128 residues, which form an obligate heterodimer with the cofactor Rrp47 (Feigenbutz et al., 2013; Schuch et al., 2014). Rrp6 containing the full C-terminus was expressed as an N-terminal His6-Smt3 fusion in *E. coli* BL21 (DE3) RIL cells with 250 µM IPTG induction for 16 hours at 18°C. Cells were harvested by centrifugation, resuspended in 1-2 volumes of 50 mM Tris-Cl pH 8.0 20% w/v sucrose, frozen in liquid nitrogen, and stored at -80°C. Prior to lysis, the suspension was thawed and adjusted to 350 mM NaCl, 20 mM imidazole, 1 mM beta-mercapto ethanol (BME), 0.1 % v/v IGEPAL CO-630, 10 µg/mL lysozyme and 10 µg/mL DNAse I. Cells were lysed by sonication with stirring on ice. The lysate was separated from unlysed cells and insoluble matter by centrifugation at 40,000 x g (4°C) for 45 min, added to Ni-NTA resin (Qiagen), and rotated for 1 hr at 4°C. Then, the resin and lysate were transferred to a disposable column, the flowthrough discarded, and the resin washed with 10 volumes of wash buffer (20 mM Tris-Cl pH 8.0, 250 mM NaCl, 20 mM imidazole, 1 mM BME) using gravity flow. The resin was then washed with 10 volumes of chaperone buffer (wash buffer plus 50 mM KCl, 10 mM $MgSO_4$, and 2 mM ATP) followed by another 5 volumes of wash buffer. Bound protein was eluted with 3 column volumes of wash buffer plus 250 mM imidazole pH 8.0 and injected onto a 5 mL Hi-Trap Heparin HP column (GE) equilibrated in 20 mM Tris-Cl pH 8.0, 250 mM NaCl, 1 mM BME. The column was washed with 4 column volumes of the equilibration buffer and eluted with a linear gradient of NaCl to 1 M over 20 column volumes. Rrp6 eluted in a peak centered at approximately 430 mM NaCl. Fractions containing the Rrp6 peak were pooled, concentrated, and digested with 1:1000 molar ratio of SUMO protease overnight at 4°C. The next day, the protein was separated from His6-Smt3 and SUMO protease using a Hiload 26/600 Superdex 200 (GE) gel filtration column (in 20 mM Tris-Cl pH 8.0, 300 mM NaCl, 2 mM BME). Fractions containing Rrp6 were pooled, concentrated to 7-10 mg/mL by centrifugation in an Amicon YM-30 filtration unit (Millipore), flash frozen in liquid nitrogen, and stored at -80°C. This protocol effectively rids the preparation of nucleic acid contamination and C-terminal truncated products. The same protocol was used to purify *E. coli* RNAse R (cloned as an N-terminal His6-Smt3 fusion), except the gradient for the heparin column was run from 250-600 mM KCl in 20 mM Tris-Cl pH 8.0, 0.1 mM $MgCl_2$, 5% v/v glycerol, 0.5 mM TCEP-HCl and the protein eluted in a peak at approximately 450 mM KCl.

HPLC purification of 3'-3' RNAs

5' alkynyl RNA oligonucleotides were synthesized and purified by standard desalting by Integrated DNA technologies. 17 and 18 nt sequences were 5' (hexynyl)UA UUA UUU AUU UUA AAA 3' and 5' (hexynyl)UUA UUA UUU AUU UUA AAA 3', respectively. Click reactions were fractionated by DEAE chromatography (Waters Protein-Pak DEAE 8HR 1000 Å 8 µm 5x50 mm column) using an Alliance 2695 HPLC separation module (Waters). The column was run at a flow-rate of 0.5 mL/min at 50°C and equilibrated in buffer A (10 mM Tris-Cl pH 8.0, 400 mM NaCl, 0.1 mM EDTA). A linear gradient to 100% buffer B (10 mM Tris-Cl pH 8.0, 600 mM NaCl, 0.1 mM EDTA) was run from 2.5 min to 30 min after injection and fractions were collected every 1 minute (Figures S1A and S1B). Fractions were analyzed by UREA-PAGE using SYBR Gold staining (Life Technologies), and those containing the desired product were adjusted to 300 mM sodium acetate pH 5.2 and 70% ethanol to precipitate the RNA. The precipitate was then pelleted by centrifugation at 20,000 x g (4°C), the solvent decanted, the pellet washed with cold 70% ethanol, centrifuged again, the solvent decanted, and the pellet air-dried for 1 hr and resuspended in approximately $1/10^{th}$ the original reaction volume of nuclease free water (Ambion). RNA concentration was calculated by measuring A_{260} using a Nanodrop 2000 and dividing that value by a theoretical extinction coefficient based on its sequence. This procedure regularly yielded 40-55% of the expected 3'-3' RNA product at concentrations of 400-550 µM.

Structure determination.
X-ray diffraction data were collected at the Advanced Photon Source 24-ID-C beam line equipped with a Pilatus-6MF detector. Data was obtained from a single crystal diffracted at a wavelength of 0.9795 Å at 100 K and processed using HKL2000 (Otwinowski and Minor, 1997). Statistics reported in Table 1 were obtained using Phenix (Adams et al., 2010). The structure was solved by molecular replacement using Phaser (McCoy et al., 2007) and coordinates of the yeast Exo10[6] (PDB: 4OO1) and yeast Rrp44 (PDB: 2WP8) as search models. The structure is refined to R/R_{free} values of 0.201/0.249. The final model includes 24 of the 34 possible nucleotides, and 3731 of the 4158 amino acids present in the crystal. Analysis of the contents of dissolved crystals is consistent with 1:1 RNA:exosome complex (Figures S1E and S1F). The asymmetric unit contains one complex. Iterative rounds of refinement were accomplished using Phenix (Adams et al., 2010). RNA and side chains were manually built using Coot (Emsley et al., 2010). Simulated annealing omit maps and maps used during building were also generated using CNS (Brunger, 2007). The model was refined using positional refinement, real-space refinement and individual B-factor refinement. Figures depicting the structure, including the surface representations in Figure 2A and the graphical abstract, were prepared with Pymol (Schrödinger). Structure quality was assessed using MolProbity (Chen et al., 2010) indicating the model has excellent geometry with 94.6% in favored, 5.2% in allowed, and 0.2% in outlier regions of Ramachandran space. The structure scored in the 100th percentile for the Clash and MolProbity scores.

RNA binding and decay assays
AU-rich RNA sequences (Integrated DNA Technologies) were A AUU AUU UAU UAU UUA UUU AUU AUU UAU UUA UUU AUU AUU UAU UUA UUA, AUU AUU UAU UUA UUA AUU AUU UAU AUU UUA UUU AUU, and AU UUA UUU AUU AUU for the 49, 36 and 14 nt RNA and were HPLC purified by Integrated DNA technologies. The sequence of the 5'-3' RNA used in Figure S1C is AAA AUU UUA UUU AUU UAU UUA UUA UUU AUU UUA AAA to mimic that of the corresponding 3'-3' RNA. Poly(A) RNAs (Dharmacon) were of the sequence A_x, where x = length in nucleotides of the indicated species, and were HPLC purified by Dharmacon. Unless otherwise noted, decay assays contained 1 nM enzyme and 10 nM RNA substrate in RNA decay buffer (20 mM Tris-Cl pH 8.0, 50 mM KCl, 0.5 mM $MgCl_2$, 0.5 mM TCEP-HCl, 0.1 % IGEPAL CO-630). For gel analysis of decay products, an aliquot of decay reactions containing 5' fluorescein or 5' 6-carboxyfluorescein (FAM) RNAs was quenched at the indicated times with an equal volume of 89 mM Tris-borate pH 8.3, 7 M Urea, 2 mM EDTA, 12% w/v Ficoll, 0.005 % w/v xylene cyanol and 10 µL was loaded onto 15% acrylamide TBE urea gels (Life Technologies). Gels were imaged for fluorescein fluorescence using a Typhoon FLA9500 instrument (GE). For measuring initial rates of decay of Exo10[44] or Rrp44 in Exo11[44/6] (Figures 3D and 4D), the Rrp44 product was quantified at the first two to three non-zero time points in triplicate using ImageJ (NIH) and converted to nM via a standard curve of fully decayed RNA. Initial rate is calculated as the slope of the linear regime of decay under these conditions. For quantification of Rrp44 activity in Exo10[44] and Exo11[44/6] complexes (Figures 3B, 3C, 4B, 4C, 4E and 4F), nM of Rrp44 product was calculated in the same fashion. For decay assays using 3' phosphate RNAs (Figures 5D and S6G), reactions were incubated at 30°C for 5 minutes in the presence or absence of 0.01 U/µL calf intestinal phosphatase (CIP, from New England Biolabs) prior to addition of the exonucleases as indicated. For K_D measurements, binding reactions (20 µL) contained 30 nM 5' FAM RNA and variable protein concentrations in RNA decay buffer. Proteins were buffer exchanged into RNA decay buffer prior to the binding experiment using Micro Biospin 6 columns (Bio-Rad). To render them catalytically inactive, Rrp44 contained D171N and D551N mutations and $Rrp6_{129-733}$ contained a D238N mutation. Reactions were incubated for 20 minutes at room temperature in black low-volume, non-binding, round-bottom 384 well plates (Corning) prior to anisotropy measurement (λ_{ex} = 495 nm, λ_{em} = 525 nm) using a Spectramax M5 plate reader (Molecular Devices). K_Ds were calculated from a triplicate measurement using eleven 1:2 serial dilutions of a given protein plus a minus protein control using a receptor depletion model to fit (Wasmuth and Lima, 2012).

References

Adams, P.D., Afonine, P.V., Bunkóczi, G., Chen, V.B., Davis, I.W., Echols, N., Headd, J.J., Hung, L.-W., Kapral, G.J., Grosse-Kunstleve, R.W., et al. (2010). PHENIX: a comprehensive Python-based system for macromolecular structure solution. Acta Crystallogr. D Biol. Crystallogr. *66*, 213–221.

Brunger, A.T. (2007). Version 1.2 of the Crystallography and NMR system. Nature Protocols *2*, 2728–2733.

Chen, V.B., Arendall, W.B., Headd, J.J., Keedy, D.A., Immormino, R.M., Kapral, G.J., Murray, L.W., Richardson, J.S., and Richardson, D.C. (2010). MolProbity: all-atom structure validation for macromolecular crystallography. Acta Crystallogr. D Biol. Crystallogr. *66*, 12–21.

Emsley, P., Lohkamp, B., Scott, W.G., and Cowtan, K. (2010). Features and development of Coot. Acta Crystallogr. D Biol. Crystallogr. *66*, 486–501.

Feigenbutz, M., Jones, R., Besong, T.M.D., Harding, S.E., and Mitchell, P. (2013). Assembly of the Yeast Exoribonuclease Rrp6 with Its Associated Cofactor Rrp47 Occurs in the Nucleus and Is Critical for the Controlled Expression of Rrp47. Journal of Biological Chemistry *288*, 15959–15970.

Greimann, J.C., and Lima, C.D. (2008). Reconstitution of RNA exosomes from human and Saccharomyces cerevisiae cloning, expression, purification, and activity assays. Meth. Enzymol. *448*, 185–210.

McCoy, A.J., Grosse-Kunstleve, R.W., Adams, P.D., Winn, M.D., Storoni, L.C., and Read, R.J. (2007). Phasercrystallographic software. J Appl Crystallogr *40*, 658–674.

Otwinowski, Z., and Minor, W. (1997). [20] Processing of X-ray diffraction data collected in oscillation mode. Meth. Enzymol. *276*, 307–326.

Schuch, B., Feigenbutz, M., Makino, D.L., Falk, S., Basquin, C., Mitchell, P., and Conti, E. (2014). The exosome-binding factors Rrp6 and Rrp47 form a composite surface for recruiting the Mtr4 helicase. The EMBO Journal *33*, 2829–2846.

Sievers, F., Wilm, A., Dineen, D., Gibson, T.J., Karplus, K., Li, W., Lopez, R., McWilliam, H., Remmert, M., ding, J.S.O., et al. (2011). Fast, scalable generation of high-quality protein multiple sequence alignments using Clustal Omega. Molecular Systems Biology *7*, 1–6.

Wasmuth, E.V., and Lima, C.D. (2012). Exo- and endoribonucleolytic activities of yeast cytoplasmic and nuclear RNA exosomes are dependent on the noncatalytic core and central channel. Mol. Cell *48*, 133–144.